Energy Systems on Autonomous Offshore Measurement Stations

Trygve Kvåle Løken

NTNU

Norwegian University
of Science and Technology

Department of Energy
and Process Engineering

EPT-M-2015-54

MASTER THESIS

for

Student Trygve Kvåle Løken

Spring 2015

Energy systems on autonomous offshore measurement stations

Energisystemer på autonome offshore målestasjoner

Statoil ASA donated a Wavescan measure buoy (WS091) to The Fluid Engineering Department at NTNU in the autumn of 2014. Later, a collaboration with Fugro OCEANOR AS (FOAS), a buoy manufacturer located in Trondheim, was initiated. Wavescan is a floating observation platform with facilities for measuring water current, wave characteristics and also wind speed direction and magnitude. Since the last couple of years, FOAS have started to deploy LiDARs on their Wavescan buoys. The LiDAR-buoys are primarily used for measurements of offshore wind profiles in conjunction with development of offshore wind farms. One of the challenges introduced by this installation is the extensive power demand of the LiDAR.

FOAS and other market participants within the remote sensing industry desires autonomous, self-running systems that can operate without costly maintenance or refueling missions. Preferably, the measurement station should be powered by means of renewable energy resources, assuring long-term data acquisition. The objective of this project is to evaluate different energy sources already available on the buoy, and resources that can be exploited in the future. The focus should be directed towards wind power.

The candidate should select a suitable small-scale turbine that will be tested in the wind tunnel at NTNU, and in the field. The field test should be conducted in a controlled environment. It is suggested that the field data is used for energy estimates at a chosen location where long-term wind data is available as open-access. Finally, the candidate should take the solar panels and fuel cells already available on the buoy into account and assess different solutions for a self-sustaining energy system.

-- " --

Within 14 days of receiving the written text on the master thesis, the candidate shall submit a research plan for his project to the department.

When the thesis is evaluated, emphasis is put on processing of the results, and that they are presented in tabular and/or graphic form in a clear manner, and that they are analyzed carefully.

The thesis should be formulated as a research report with summary both in English and Norwegian, conclusion, literature references, table of contents etc. During the preparation of the text, the candidate should make an effort to produce a well-structured and easily readable report. In order to ease the evaluation of the thesis, it is important that the cross-references are correct. In the making of the report, strong emphasis should be placed on both a thorough discussion of the results and an orderly presentation.

The candidate is requested to initiate and keep close contact with his/her academic supervisor(s) throughout the working period. The candidate must follow the rules and regulations of NTNU as well as passive directions given by the Department of Energy and Process Engineering.

Risk assessment of the candidate's work shall be carried out according to the department's procedures. The risk assessment must be documented and included as part of the final report. Events related to the candidate's work adversely affecting the health, safety or security, must be documented and included as part of the final report. If the documentation on risk assessment represents a large number of pages, the full version is to be submitted electronically to the supervisor and an excerpt is included in the report.

Pursuant to "Regulations concerning the supplementary provisions to the technology study program/Master of Science" at NTNU §20, the Department reserves the permission to utilize all the results and data for teaching and research purposes as well as in future publications.

The final report is to be submitted digitally in DAIM. An executive summary of the thesis including title, student's name, supervisor's name, year, department name, and NTNU's logo and name, shall be submitted to the department as a separate pdf file. Based on an agreement with the supervisor, the final report and other material and documents may be given to the supervisor in digital format.

☐ Work to be done in lab (Water power lab, Fluids engineering lab, Thermal engineering lab)
☒ Field work

Department of Energy and Process Engineering, 14. January 2015

Olav Bolland
Department Head

Lars Sætran
Academic Supervisor

Energy systems on autonomous offshore measurement stations

Trygve Kvåle Løken

Norwegian University of Science and Technology, Dept. of Energy and Process Engineering, 7491 Trondheim

Abstract

In this study, a performance test has been performed on a 200 W marine wind turbine, both in the wind tunnel at The Fluid Engineering Department at the Norwegian University of Science and Technology, and mounted on a Wavescan measure buoy in a coastal location near Trondheim. Long term wind data satisfying the DNV-RP-C205 recommended practice for describing environmental conditions and environmental loads have been extracted from the Eklima database subordinated the Norwegian Meteorological Institute for a selected location called Sula weather station outside of the Norwegian coast. 10 years of data from Sula and a one-month performance test near Trondheim formed the basis for monthly wind energy estimates at the Sula site. Energy estimates for solar production on the Wavescan has been carried out at the same site utilizing a solar engineering software called Meteonorm.

The motivation of the study is to ensure continuous energy supply on remote measurement station enabling one-year autonomous operation. This criterion has proven obtainable at the selected site with an energy system consisting of the solar panels and fuel cells already installed on the standard Wavescan buoys combined with an Air Breeze wind turbine. An alternative solution relying solely on renewable energy resources is to increase the turbine rotor area by 85%, or to introduce a second turbine.

1. Introduction

Fugro Oceanor AS (FOAS) is a buoy manufacturer located in Trondheim. Their main product is the Wavescan buoy. The Wavescan is a floating observation platform with facilities for measuring water current, wave characteristics and also wind speed direction and magnitude. Since the last couple of years, FOAS has started to deploy lidars on their Wavescan buoys. The lidar-buoys are primarily used for measurement of offshore wind profiles in conjunction with development of offshore wind farms. One of the challenges introduced is the extensive power demand of the lidar.

The lidar applied is the ZephIR 300 which has a monthly energy consumption of 50 kWh [1] on average. The overall monthly energy consumption of the lidar and the rest of the buoy is 52 kWh [2]. Wavescan buoys are usually equipped with four Solara solar panels for power generation. The panels generate 7.5 kWh on average on a monthly base when located in the Norwegian Sea outside of Trondheim. Four chargeable Powersafe lead acid batteries and four Saft lithium backup batteries are installed. The total battery capacity is approximately 13 kWh [2]. In order to make balance in the energy budget, FOAS has installed four Efoy Pro 2400 Duo methanol fuel cells capable of sustaining buoy operation for approximately six months without refueling, combined with solar and batteries.

A small scale wind turbine will be selected for testing, first in the wind tunnel at the Norwegian University of Science and Technology (NTNU) and later in the field, mounted on the Wavescan buoy. The system will be tested under controlled conditions outside of the pier in the Trondheim fjord at the test site of FOAS. The field test will be used as a base to estimate energy production at a chosen location where long-term wind and solar irradiation data is available as open-access. Finally, the solar panels and fuel cells already available on the buoy will be taken into account and different solutions for a self-sustaining energy system will be discussed.

1.1 Wind profile

Wind speed varies with time and height above the sea surface. Therefore, it is important to specify the reference height H where the measurement is done, and the averaging time for the wind speed. According to DNV-RP-C205 recommended practice for describing environmental conditions and environmental loads [3], the wind climate of a certain site can be expressed in terms of the 10-minute mean wind velocity $U(H)$ at the reference height. The wind velocities occurring within 10 minutes can be considered normally distributed around the mean with a given standard deviation σ, which describes the turbulence in the wind. If one wish to know the wind velocity at a certain elevation z, one should correct the velocity at the reference elevation according to the wind profile. Correction is especially important close to the sea surface, even for small elevation differences, due to the sharp gradient of the wind profile close to the surface. A commonly used wind profile model is the logarithmic profile which can be written as following [3]:

$$U(z) = U(H)\left(1 + \frac{\ln(z/H)}{\ln(H/z_0)}\right) \tag{1}$$

where z_0 is a roughness parameter that depends on the wave height, which in turn depends on the wind velocity [4]. For offshore locations, the roughness parameter can be solved implicitly from the following equation:

$$z_0 = \frac{A_C}{g}\left(\frac{k_a U(z)}{\ln(z/z_0)}\right) \tag{2}$$

where g is the acceleration of gravity and $A_C = 0{,}018$ is Charnock's constant for near-coastal locations [3]. $U(H)$ is used as an approximation for $U(z)$ when solving this equation.

1.2 Wind distribution

Empirical and statistical data are used to describe the wind climate at a given location. Site-specific, measured wind data over sufficiently long periods of time with minimum gaps of lacking data are preferable. For design purposes, a 10-year period or more of continuous data is recommended [3]. Usually, a sample of $U(H)$ spanning over several years is representative as a basis for estimation of the cumulative distribution function of the velocity (Eq. (3)).

Once the mean wind velocity has been corrected with respect to the wind profile, one can model a wind distribution for the site. A wind distribution is a histogram that shows the frequency of discrete wind velocity ranges within the sample and can cover a whole year or shorter periods.

The cumulative distribution function $F(U) = p(U' \leq U)$ states the probability of a random wind velocity U' being smaller than a given wind velocity U, and is defined as:

$$F(U) = \int_0^U p(U')dU' \tag{3}$$

where $p(U')$ is the probability density function stating the probability of U' occurring. Common probability distributions used in the area of wind engineering is Rayleigh, Weibull and Gumbel. Normally, the Weibull distribution gives the best results [5, 6]. The Weibull cumulative probability function is defined as:

$$F(U) = 1 - e^{-\left(\frac{U}{c}\right)^k} \tag{4}$$

where k is a shape factor and c is a scale factor. These parameters can be found from a wind distribution by rearranging Eq. (4):

$$\ln\left(\ln\left(\frac{1}{1-F(U)}\right)\right) = k \ln U - k \ln C \tag{5}$$

as showed in [7]. This equation is now on the general slope-intercept form $y = ax + b$. Now, $\ln U$ and $\ln[\ln(1/[1 - F(U)])]$ can be calculated for each velocity and plotted on the x-axis and the y-axis respectively. A linear least squares solver calculates the slope and the intercept with the y-axis of the line of best fit. k is the slope of this line, and c is equal to $\exp(-intercept/slope)$.

1.3 Wind power

Wind turbines harvest kinetic energy in the wind and converts it into electrical energy. Flow over airfoils creates lift forces on the blades that induces a torque on the rotor. The performance of a turbine is characterized by the power coefficient C_P which is equal to generated, mechanical power P_{mech} divided by available wind power:

$$C_P = \frac{P_{mech}}{\frac{1}{2}\rho \cdot A \cdot U^3} \tag{6}$$

where ρ is the air density and A is the rotor area. The theoretically maximum possible power coefficient of a wind turbine is the Betz limit equal to 0.59, derived through annular stream tube control volume analysis as shown in [8]. The thrust force in the wind is defined as:

$$T = \frac{1}{2} \cdot \rho \cdot A \cdot U^2 \tag{7}$$

Every wind turbine has a characteristic power performance curve $P_w(U)$ that varies with the wind velocity. Performance is maximized between cut-in speed, which is the minimum wind speed required to generate power, and the rated wind speed, where maximum power output occur. The performance curve has typically a cubic shape in this region, since the wind power is proportional to wind speed cubed as seen in Eq. (6). Above rated wind speed, the performance is limited,

typically with pitch control on full-scale turbines. The power curve is ideally constant in this region until cut-out speed is reached and production ceases.

The average power production of the turbine $\bar{P}_w$ can be found if the wind distribution or the probability distribution function $p(U)$ of the location is known:

$$\bar{P}_w = \int_0^\infty P_w(U)p(U)dU \qquad (8)$$

Here, $\bar{P}_w$ can be the average of a year, a season or a month, corresponding to the span of the probability distribution [5].

2. Methods

2.1 Air Breeze [9]

Several turbines were purchased and available for deployment on the buoy. For details, see Appendix A. The choice fell to Air Breeze due to its low weight and good performance relative to the competitors. Air Breeze is a three-bladed battery charging wind turbine used in remote, off-grid locations such as sailboats and monitoring stations. It is coated with a corrosion resistant paint for marine applications. The turbine has a three-phase brushless permanent magnet generator and a microprocessor-based smart controller. A rectifier converts the voltage to DC ahead of the battery terminals, and a potentiometer monitors the battery voltage. The long tail fin and yaw shaft allows for passive yaw control. A sketch of the turbine is presented in Appendix B.

In charging mode, the controller optimizes the power production capacity by continuously adjusting the alternator loading, and thus the stator voltage, which is directly proportional to the rotational speed of the turbine. This means that the wind turbine operates at its best performance, independent of the external load and the system voltage. Below rated wind speed, the rotational speed is controlled to keep the blades operating at the optimal angle of attack in order to ensure maximum energy extraction. Above rated wind speed, over-speed protection is activated. The controller restrains power production by limiting the rotational speed by means of electronic torque control.

2.2 Wind tunnel test

The wind turbine was tested in the wind tunnel at NTNU to validate the credibility of the turbine performance presented on the web page of the manufacturer and here in Appendix C. The graph shows a typical cubic power curve up to a rated wind speed of 11 m/s where power output peaks with approximately 250 W [10]. For higher wind speeds, the power is constantly 200 W.

The experimental set-up presented in Fig. 1 resembled the planned buoy configuration, where the wind turbine was wired to a battery bank and a thermal load that dissipated produced energy. The battery bank consisted of four 90 Ah PowerSafe lead acid batteries. Sensors measured charging parameters, thrust force, wind velocity and turbine rpm. Analogous signals from the sensors were digitalized in a DAQ-box connected to a field computer. LabView was used to log the signals from the different sensors. Starting with zero flow, the velocity was increased up to a maximum velocity of 18 m/s. For each velocity, a 20 seconds, 50 Hz measurement was carried out. Each parameter was averaged over the period.
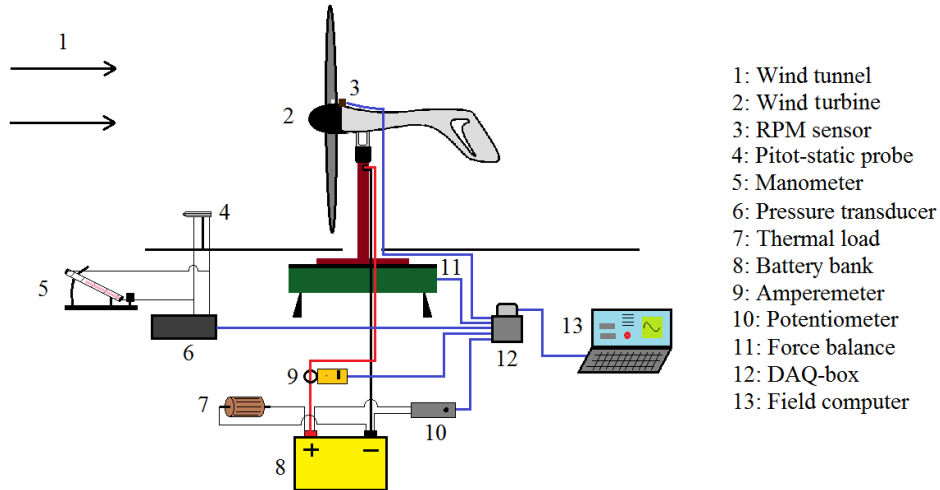
Fig. 1: Wind tunnel test set-up

Air velocity U was measured with a Pitot-static probe placed in front of the turbine. The alcohol manometer was a reference for calibration of the pressure transducer. For calibration details, see Appendix D. The turbine was mounted on a tower, which in turn was fixed to a force balance that measured the thrust exerted on the turbine. A photo sensor mounted on the nacelle, facing the rotor plane counted the rotational speed by sensing a reflecting tape attached to one of the blades. Electric current flowing from the turbine to the battery was measured with an ammeter clamped around the positive conductor of the turbine. System voltage was measured with a potentiometer connected in parallel with the battery. It turned out more convenient to measure electrical power compared to mechanical power as the turbine drive shaft was sealed in the turbine house casing, making it impossible to connect it to a torque gauge. Additionally, this solution made the lab test and the field test compatible since the buoy configuration would log current consumption and production, which is directly proportional to electric power. A thermal load was connected in parallel with the battery with the purpose of dissipating energy at a rate approximately matching the energy production of the turbine. The electrical resistance of the thermal load selected was 2 Ω, which is a compromise between heat emission and estimated power output from the turbine

2.3 Buoy configuration

Regular Wavescan buoys have one mast with a sensor carrier assembly on top, supporting the ultrasonic wind sensor 4.0 m above the sea surface. The Air Breeze turbine was mounted on top of a second mast, with a resultant hub height of 2.6 m above the sea surface. The wind velocity measurements were elevation-corrected to the hub height according to the logarithmic profile by means of Eq. (1) and (2). The velocity difference was significant; 4% decrease at 5 m/s and 5% decrease at 10 m/s. The arrangement, seen in Fig. 2, yielded a vertical clearance of approximately 0.8 m and a horizontal clearance of 1.3 m between the top of the rotor plane and the wind sensor. According to Krogstad et al. [11], the wake area behind a turbine expands with approximately 50% in a distance of one rotor diameter (which in this case is equal to 1.15 m) downstream of the rotor plane. Hence, the vertical clearance for the wind sensor to avoid the wake of the turbine in the case where the turbine is oriented upstream of the wind sensor is sufficient.
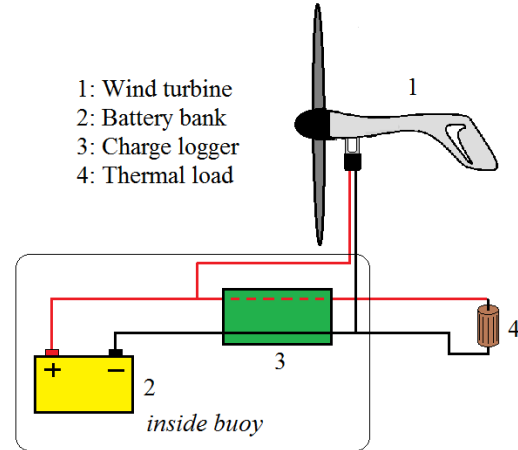
Fig. 2: Turbine on buoy   Fig. 3: Electrical configuration on buoy

The wind turbine and its complementary electrical system shown in Fig. 3 was wired isolated from the rest of the buoy in order to reduce sources of error that could disturb the measurements. The turbine was connected to a battery bank and a charge logger was used to monitor current flowing to and from the battery. In the future, the wind turbine is intended to supply sensors on board with energy. However, this set-up was just a preliminary test and no functional equipment would consume the produced power. A thermal load, similar to the one used in the lab set-up, was applied to dissipate produced energy and prevent the batteries from filling up.

The meteorological parameters on a Wavescan buoy are usually sampled once an hour with 1 Hz sampling rate averaged across 10 minutes. It was desirable to get as detailed information as possible regarding the performance of the wind turbine. Therefore, the acquisition interval of the wind parameters (direction and velocity) was decreased to 10 minutes. The same time resolution was chosen for the charge logger.

The charge logger had an internal switch that disconnected the load when the battery voltage dropped below 11.6 V to prevent the load from emptying the battery, typically during a calm period when little energy was generated. The load was reconnected when the voltage increased above 12.6 V.

2.4 Solar panels

Solar panels converts light into electricity through the photovoltaic effect. The radiation intensity of the sunlight determines the amount of energy available for harvest, along with the efficiency and area of the solar cells. The radiation parameter used for energy estimates is the global radiation intensity $[W/m^2]$, which is the sum of direct B and diffuse D radiation.

Meteonorm, which is a database containing climatological data for solar engineering applications, was applied to estimate the monthly global radiation subjected to the solar panels on the buoy, when located at Sula weather station. For further details about Meteonorm, see [12]. Site-specific parameters used as initial conditions in the simulation are listed in Appendix E.

The buoy has four Solara SM 160M solar cells, each with an area of 0.40 m^2. The effective area of the monocrystalline wafers on each panel, excluding the assembly is 0.24 m^2, making a total effective area of 0.96 m^2. Since the buoy has four solar panels and the orientation of the buoy is arbitrary and unknown, it was assumed that each solar panel faces different orientations on average. That is, one panel face south, another face west, and so on. One simulation was carried out for each

panel, and the sum of irradiation density was multiplied with the total effective area of the solar panels.

SunWays Photovoltaic Technology delivers a solar panel with an effective area of $0.5625\ m^2$. According to [13], these panels have an approximately linear correlation of $0.005\ A/[W/m^2]$ between generated current and irradiation density. For further details, see Appendix F. The panels on the buoy are of a different brand, but the same cells are used, hence the same data sheet is applicable [14]. Monthly energy estimates are calculated with the following formula:

$$E_{SOLAR}\left[\frac{kWh}{month}\right] = x\left[\frac{kWh}{m^2\cdot month}\right]\cdot 0.005\left[\frac{A}{W/m^2}\right]\cdot \frac{1}{0.5625\left[m^2\right]}\cdot Area\left[m^2\right]\cdot 12\left[V\right] \qquad (9)$$

where x is the Global irradiation density extracted from Meteonorm, $Area = 0.96$ is the effective area of the cells installed on the buoy and $12\ V$ is the system voltage onboard the buoy.

2.5 Fuel cells

Fuel cells transform chemical energy into electricity via a redox reaction. Four Efoy Pro 2400 Duo fuel cells fueled with methanol are usually installed on the lidar-buoys. Taking the heating value of the chemical reaction (Eq. (10)) and the efficiency of the cells into account, the cells consumes 0.9 l of fuel for every produced kWh of electric energy [15]. The following overall reaction takes place inside the cells:

$$CH_3OH + \frac{3}{2}O_2 \rightarrow 2H_2O + CO_2 \qquad (10)$$
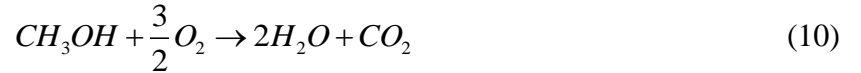
The fuel cells are placed in four small compartments cut out in the hull. Two of the cells are supplied with three fuel cartridges and the other two are supplied with two. There are in total ten fuel cartridges containing 28 l each, yielding a total fuel volume of 280 l. More fuel cells would extend the lifetime of the buoy, but the structural integrity of the hull cannot allow for any more cartridges. The fuel cells are activated when the battery voltage drops below a specified limit of 12.3 V and operates until the battery is fully charged and the voltage has increased above 14 V.

3. Results and discussion

3.1 Power performance

Fig. 4 shows the power curve (blue) and the power coefficient of the turbine (red) plotted versus the wind velocity. During the wind tunnel test, the power output reached a maximum value of 186 W at 10.5 m/s. The rotational speed of the turbine increased from 600 rpm at cut-in speed, up to 1000 rpm at maximum output. The controller entered over-speed protection as the wind velocity exceeded 11 m/s, and consequently, the rotational speed decreased to approximately 800 rpm. When comparing the power curve with the one in the data sheet presented by the supplier (Appendix C), one can see a more or less corresponding behavior. However, the power output under ideal conditions in the wind tunnel was 28% lower than promised in the data sheet at rated wind speed. The output was approximately 120 W for velocities above rated wind speed, 40% lower than promised, which is a significant difference.

By definition, the power coefficient is mechanical power on the drive shaft over power content in the wind. Electrical power is slightly lower due to generator losses and losses introduced by power electronics. These losses are typically 5-10% for a brushless permanent magnet generator [16]. Since the calculated power coefficient presented in Fig. 4 is based on electrical power output, this indicates a slightly higher mechanical power coefficient. The best electrical power coefficient achieved in the wind tunnel test was 41% at 7 m/s; hence, the mechanical power coefficient was probably around 44%. This is a plausible value compared to the Betz limit, and a good value considering that commercial, full-scale turbines have an efficiency up to 45-50% [17].
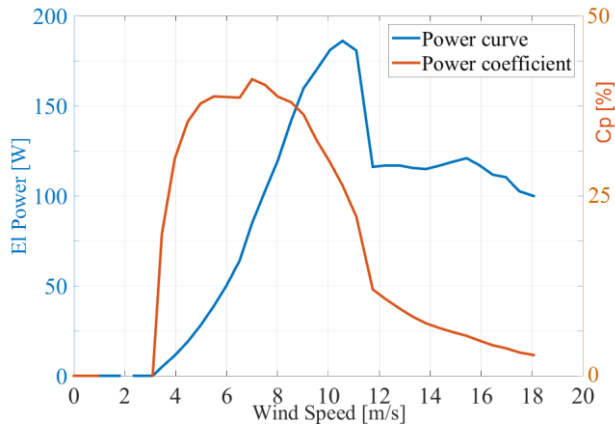
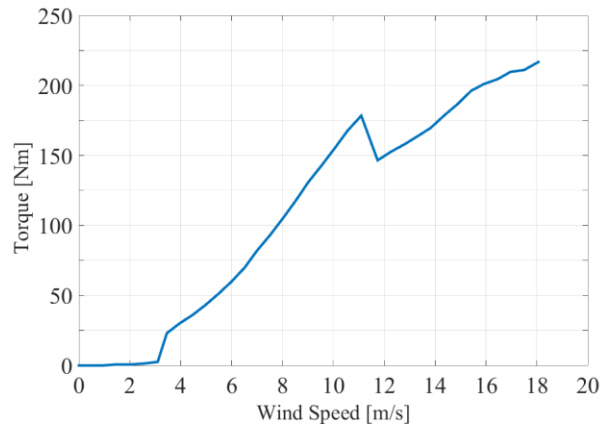Fig. 4: Electric power and power coefficient

Fig. 5: Torque

The main sensor of the Wavescan has traditionally been the wave sensor, which consists of accelerometers and gyroscopic moment sensors. If the wind turbine should be incorporated into the energy system of the buoy, it should be considered that this torque could change the dynamic response of the turbine, and affect buoy motion and thus the wave measurements. Fig. 5 shows the thrust force subjected on the turbine by the wind multiplied by the distance from the turbine to the rotational axis of the buoy. The drag force on the tower is not accounted for in this plot. At 10.5 m/s, the buoy would be subjected to a 175 Nm torque.

The turbine was tested on a buoy located outside of Munkholmen in the Trondheim fjord. The test period spanned from April 13th till May 25th 2015, with a gap of 10 days from May 8th, due to a malfunction on the wind sensor. The configuration worked out well during the field test, except that while the load was disconnected, the charge logger did not record any charging even though the measured wind velocity would indicate that the turbine was generating power. Therefore, all data acquired while the load was disconnected, was discarded. As soon as the load was reconnected, all data was logged as usual.
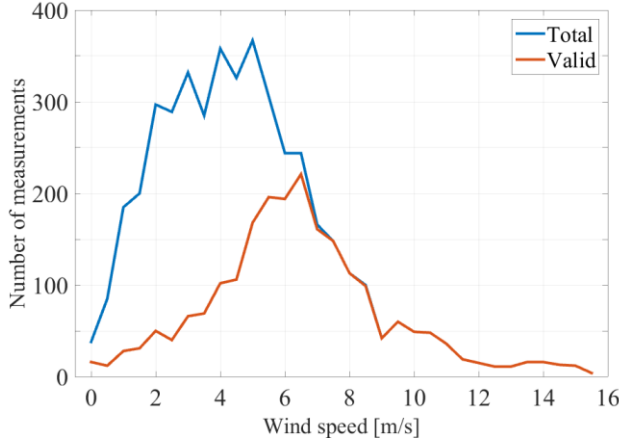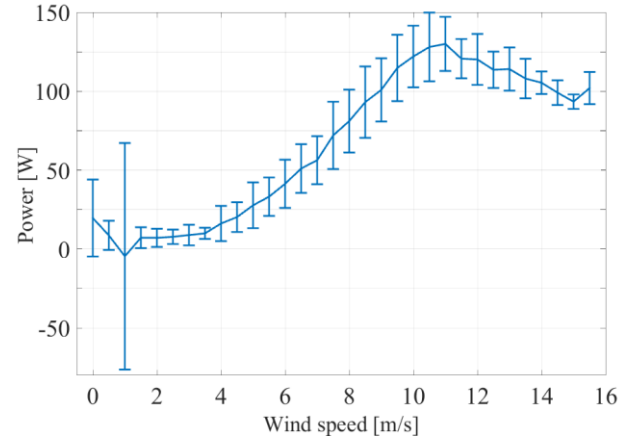
Fig. 6: Valid power data

Fig. 7: Power curve with standard deviation

Fig. 6 show the number of total and valid 10-minute measurements at each wind speed. 50% of the data was discarded in total due to the charge logger error. Fig. 7 shows the average electric power output, including the standard deviation of all the measurements at each wind speed plotted as error bars. A high uncertainty was related to the measured values for velocities up to 1.5 m/s. These measurements were therefore neglected.
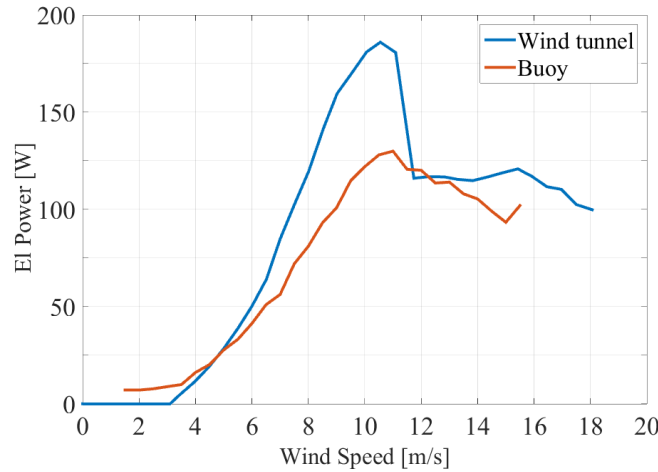

Fig. 8: Electric power-output in the wind tunnel (blue) and in the field (red)

The logged wind velocities were sorted into bins of resolution equal to 0.5 m/s, and the power produced at each wind speed was averaged and allocated to the respective bin. Fig. 8 show a qualitative consistence between the electric power output from the wind tunnel test (blue) compared with the results from the test period on the buoy (red). The power output from the buoy peaked at 128 W. From cut-in speed up to rated wind speed, the output was approximately 35% lower than expected during ideal conditions. Above rated wind speed however, the difference in power output was less significant. The power curve from the tunnel test had a sharp peak and a steep drop as the over-speed protection was activated. The power curve from the buoy test had a much smoother drop due to hysteresis around the control point within a 10-minute average period. The highest recorded wind speed from the period was 15.5 m/s. For energy estimates, a constant power output of 100 W was assumed for wind speeds reaching from 15.5 m/s to cut-out speed at 22 m/s, based on the results presented in Fig. 8.

There could be several explanations for why the turbine had a lower performance in the field compared with the laboratory test. According to wave measurements from the same site collected from December 16th 2014 till January 28th 2015, the rotor area perpendicular to the wind speed is on average insignificantly reduced as the turbine is subjected to buoy motion. However, as the buoy rolls and pitches, the angle of attack of the blades constantly deviates from the optimum value. This suboptimal aerodynamic performance decreases the turbine efficiency.

The conditions in the field were transient and one might expect better performance during laminar conditions in the wind tunnel. However, turbulent wind conditions could indicate a higher power output due to an increased kinetic energy flux during a 10 minute averaging period compared to a steady mean wind [18]. This only applies if the turbine has a quick response and is able to utilize the turbulent energy in the wind. Deeming from the power curves presented in Fig. 8, it appears as if the Air Breeze is unable to benefit from the turbulent energy, and that turbulent wind conditions undermine the power production.

3.2 Sula

Eklima is a web service subordinated the Norwegian Institute of Meteorology. It offers long term wind data from numerous weather stations around the country. Sula lighthouse was chosen because it is located on a small island exposed to the ocean in all orientations, and it represents a climate similar to what an ocean buoy typically is subjected to. It is emphasized that the results only apply for this specific location as wind conditions vary geographically. If the buoy is deployed at other sites, new estimates should be carried out.

A ten-year sample spanning from March 2005 was extracted from the Eklima database [19]. The sample contained 10-minutes averaged wind velocity data with one-hour acquisition intervals. A two-month period from December 2008 until February 2009 contained no data. Except for this short disruption, the data quality was adequate.
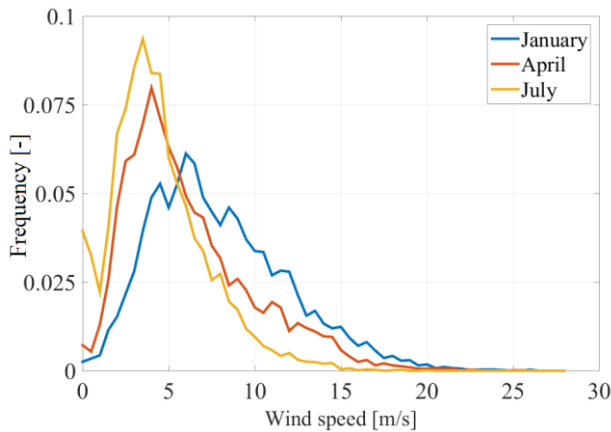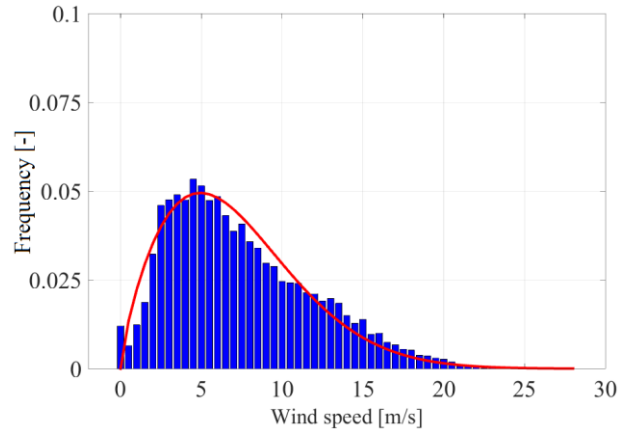

Fig. 9: Wind distributions   Fig. 10: Weibull fit for average March

The data was divided into months, and the occurrence frequency of each wind speed bin (resolution equal to 0.5 m/s) within each month was logged. Fig. 9 shows the ten year averaged, monthly wind distributions for three selected months. Higher wind speeds were more frequent in January compared to April, and July had the lowest average wind speed.

Since the sample spanned over several years, the wind distributions could be considered as representative probability density functions [3]. The cumulative distribution function was

estimated for each averaged month according to Eq. (3). Then, the Weibull parameters for each averaged month were calculated according to Eq. (5). As an example, the wind distribution and the fitted Weibull distribution for March are plotted in Fig. 10. The two distributions were quite consistent, thus the Weibull distribution was a reasonable assumption. This example was included to illustrate how the Weibull distribution can be applied when corresponding parameters are available at a given site, and long-term data is not [4].

3.3 Energy estimates

The power data acquired on the buoy were primarily dependent on the wind speed. Site-specific wind conditions and turbulence could affect the behavior of the turbine, but these parameters were neglected as they were out of the complexity scope of this study. The power curve was therefore assumed applicable for power estimates at any location. Average wind power production on a monthly base at Sula was estimated with Eq. (8). Solar production on the buoy was estimated with Eq. (9), and with irradiation data from the Meteonorm software for the same site. The results are presented in Fig. 11 along with solar and wind combined.
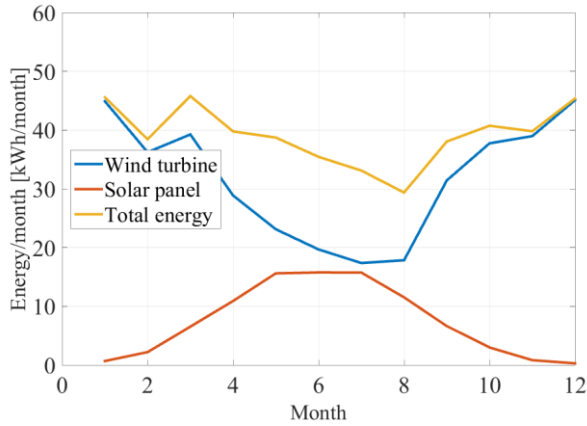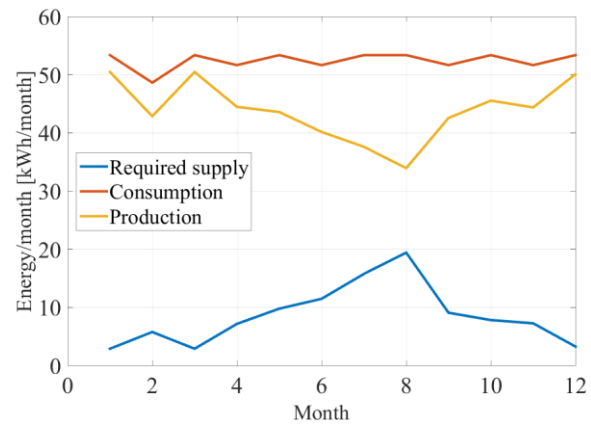

Fig. 11: Monthly energy production

Fig. 12: Monthly energy budget

In the winter months, estimated wind production was high; 45 kWh in December and January, and solar production was close to zero. Towards the summer months, solar power production increased in opposite phase with decreasing wind power production. Seasonal changes yielded more or less constant renewable energy resources throughout the year. These estimates suggested a monthly production of approximately 40 kWh on average.

When comparing total renewable energy production with energy consumption onboard the buoy, presented in Fig. 12, the outcome was not a balanced energy budget. The figure shows a monthly additional energy requirement of 13 kWh on average, less in the winter and more in the summer. This requirement could be met with the use of fuel cells. According to the nominal capacity of the fuel cells and the total fuel storage, the buoy could operate autonomous for 24 months at this specific location when solar, wind and fuel cells are combined. As a safety factor, these estimates do not take battery capacity into account. The battery should only be considered as a buffer for daily or weekly fluctuations of solar and wind availability.

4. Conclusion

Using a wind turbine for power generation on the Wavescan buoy has proven successful. Qualitatively, the same power curve was obtained in the field test as under ideal conditions in the wind tunnel. The deviations were most likely due to transient conditions and change of angle of attack on the blades as the buoy was subjected to wave motion. Also, the charge logger did not operate satisfactory. A preliminary laboratory test did not reveal the failure, therefore an extensive quality test should be carried out in the future before deployment to a long-term test.

Wind turbine deployment on offshore measurement stations offers the obvious benefit of high wind resource availability. A negative consequence could be turbine wear due to extreme wind conditions, icing and salt. These uncertainties are not accounted for in this study, as the turbine was only tested for one and a half months.

As a conclusion, an energy system consisting of the solar panels and fuel cells already installed on the standard Wavescan buoys combined with an Air Breeze wind turbine would ensure autonomous operation for 24 months at the selected site, which is a significant improvement compared to the current 6 months operation capability. An alternative solution could be a supply system based solely on renewable energy. Increased solar panel area might prove difficult due to space limitations. A more convenient solution is increased turbine rotor area. The turbine area would have to be increased by 85% in order to balance the energy budget throughout the year, assuming a linear correlation between rotor area and power output. Alternatively, a second turbine could be introduced. In that case, it is recommended to mount the turbines at different elevations to avoid wake losses when the turbines are aligned with the wind speed direction, and to consider thrust data imparted on the buoy.

Acknowledgements

Risk assessment

The project work has been carried out at two potentially hazardous locations; the assembly hall of Fugro Oceanor AS and on board Trondheim Boatman Marine Operations service ship. The Occupational Health and Safety Management System of Fugro Oceanor AS is assessed by Dovre Certification AS, and is concluded to comply with the SN-BS OHSAS 18001 – 2007 standard. Trondheim Boatman have their own health and safety regulations that requires use of life wests and helmets at all times onboard. The ship is also equipped with survival suits and a first aid kit.

References

[1]   (2015) Spec Sheet - ZephIR lidar. *Zephir Ltd.*
[2]   (2010) User Manual - Wavescan buoy WS091. *Fugro Oceanor AS*.
[3]   "Environmental Conditions and Environmental Loads," *DNV-RP-C205,* 2014.
[4]   H. Bredemose, S. E. Larsen, D. Matha, A. Rettenmeier, E. Marino, and L. R. Sætran, "Offshore wind-wave climates and their scaling to lab conditions," *MARINET,* pp. 11-15, 2012.
[5]   J. F. Manwell, J. G. McGowan, and A. L. Rogers, *Wind Energy explained: theory, design and applications*, 2nd ed. Chichester: Wiley, 2009.

[6]   J. P. Hennessey Jr., "Some Aspects of Wind Power Statistics," *Journal of Applied Meteorology and Climatology,* vol. 16, pp. 119-128, 1977.

[7]   N. L. Johnson, S. Kotz, and N. Balakrishnan, *Continuous Univariate Distributions* vol. 1. New York: Wiley Interscience 1994.

[8]   E. Kulunk and R. Carriveau, *Aerodynamics of Wind Turbines, Fundamental and Advanced Topics in Wind Power*: InTech, 2011.

[9]   "User manual - Air Breeze," *Southwest Windpower, Inc.,* 2008.

[10]   (2013) Spec Sheet - Air Breeze. *Primus Windpower.*

[11]   P. Å. Krogstad and P. E. Eriksen, "Blind Test, calculations of the performance and wake development for a model wind turbine," *Renewable Energy,* vol. 50, pp. 325-333, 2012.

[12]   "Handbook part II: Theory," *Meteonorm,* vol. Version 7.1, 2014.

[13]   (2009) Data sheet - Sunways Solar Cells. *Sunways Photovoltaic Technology.*

[14]   (2010) Data sheet - Solara M-Serie/s. *Centrosolar AG.*

[15]   (2013) Data sheet - EFOY Pro Fuel Cells. *SFC Energy.*

[16]   D. G. Dorrell, "Design Requirements for Brushless Permanent Magnet Generators for Use in Small Renewable Energy Systems," presented at the 33rd Annual Conference of the IEEE, Taipei, 2007.

[17]   T. e. a. Burton, *Wind Energy Handbook*: JonWiley and Sons, 2001.

[18]   L. M. Bardal, L. R. Sætran, and E. Wangsness, "Performance test of a 3MW wind turbine - effects of shear and turbulence," *Energy Procedia, 2015*

[19]   http://sharki.oslo.dnmi.no/portal/page?_pageid=73, 73_39049&_dad=portal&_schema=PORTAL. (2015, May 3rd). *Eklima.*
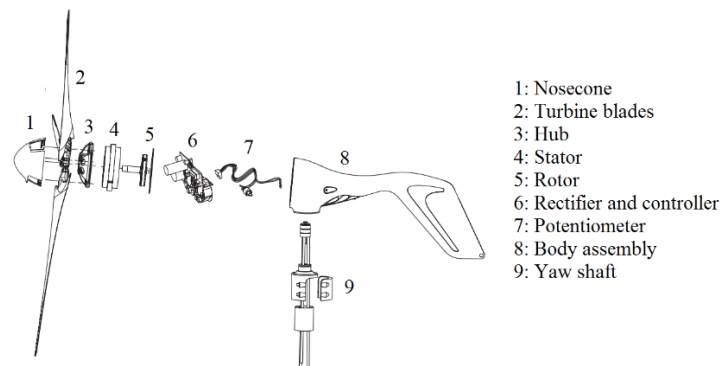
Appendix A

Turbine parameters	Air Breeze	D400 Industrial	Ampair 100	WS-015
Swept area [m^2]	1.04	0.95	0.93	0.15
Weight [kg]	6	17	12.5	38
Rated power [W] at x [m/s]	250 at 11	420 at 14	60 at 10	70 at 40
Cut-out speed [m/s]	22	-	-	40
Number of blades	3	5	6	-
Axis	Horizontal	Horizontal	Horizontal	Vertical

Turbine parameters for assessed models [1-5]

Four turbines were purchased and ready for deployment on the buoy. The choice fell to Air Breeze due to its low weight and good performance relative to the competitors.
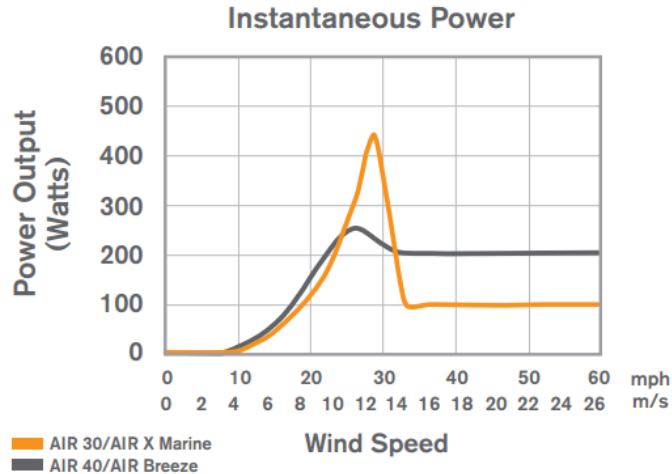
Appendix B

1: Nosecone
2: Turbine blades
3: Hub
4: Stator
5: Rotor
6: Rectifier and controller
7: Potentiometer
8: Body assembly
9: Yaw shaft

Air Breeze assembly [3]

The Air Breeze turbine has a three-phase brushless permanent magnet generator and a microprocessor-based smart controller. A rectifier converts the voltage to DC ahead of the battery terminals, and a potentiometer monitors the battery voltage. The long tail fin and yaw shaft allows for passive yaw control.

Appendix C

Air Breeze power curve (black) presented by the producer [4]

The graph shows a typical cubic power curve up to a rated wind speed of 11 m/s where power output peaks with approximately 250 W. For higher wind speeds, the power is constantly 200 W.
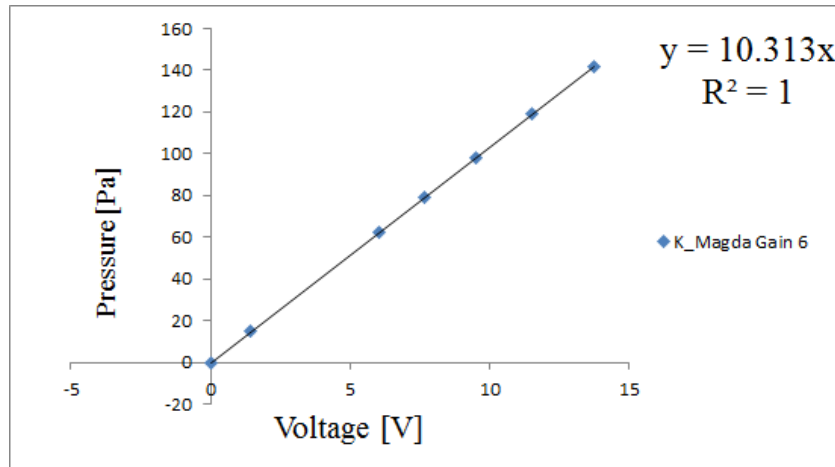
Appendix D

The velocity U was indirectly measured with a Pitot-static probe, which measures the difference between stagnation pressure P_{stag} and static pressure P. The velocity is then calculated with the Bernoulli equation:

$$U = \sqrt{\frac{2\left(P_{stag} - P\right)}{\rho}} \tag{1}$$

The alcohol manometer was a reference for calibration of the pressure transducer that converted the signal into voltage. For calibration, pressure read from the manometer was plotted against voltage read from the pressure transducer. Before the experiment was conducted, the Pitot-static probe was leveled and exposed to a high wind velocity. This was done to let the alcohol inside the manometer moist the inner perimeter of the entire scale in order to avoid capillary resistance in the manometer during the experiment. The slope of the line obtained through linear regression was the calibration constant K [Pa/V]. The calibration constant was found to be 8.24 Pa/V.

It should be mentioned that some problems were encountered during calibration of the pressure transducer used for velocity measurements, probably due to an inaccurate alcohol manometer. The results were obviously wrong since a power coefficient very close to the Betz limit was obtained, which indicates low velocity measurements. Previous experiments [6] have concluded that the calibration constant for the very same transducer amplified with the same gain is 10.31 Pa/V. This error was discovered at after the wind turbine was installed on the buoy and the narrow time window did not allow for a second wind tunnel test. Therefore, the results were corrected post experimentally with the well-established coefficient.

Kalibration of pressure transducer "Magda" [6]

Appendix E

Parameter	Value
Latitude	63,8467 [deg]
Longitude	8,4667 [deg]
Measure period	1999-2010
Inclination	18 [deg]
Azimuth	0/ 90/ 180/ -90 [deg]
Effective area	0,24 [m^2]
Irradiation	Global, interpolated
Measure stations	Østersund (S), Umeå (S)
Albedo	15 [%]
Horizon	None
Situation	Sea/ lake
Turbidity	Interpolated

Specifications used in Meteonorm

Azimuth is the angle between south and the orientation of the solar panels. The site chosen is Sula weather station. Albedo is the reflectivity of the surroundings, the chosen value was recommended for water in [7]. Turbidity is a measure of particles in the air blocking the incoming radiation. Its value was interpolated from nearby measurement stations.

Appendix F
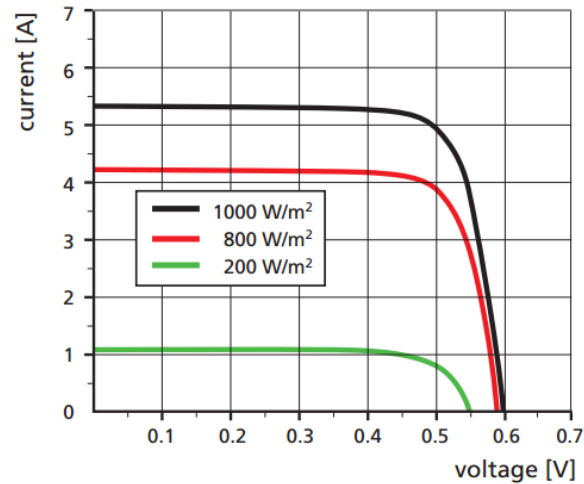
IV behavior at various degrees of irradiation intensity [8]

The graph show the IV curves of a solar panel delivered by SunWays Photovoltaic Technology. According to the diagram, there is an approximately linear correlation of $0.005 \, A/[W/m^2]$ between generated current and irradiation density over a wide range of voltages. This correlation is used for solar power estimates.

Appendix References

[1]   Spec Sheet - D400 Industrial. *Eclectic Energy Ltd.* .
[2]   (2007) Technical Data Sheet - WS-015 *Windside Production Ltd.*
[3]   "User manual - Air Breeze," *Southwest Windpower, Inc.,* 2008.
[4]   (2013) Spec Sheet - Air Breeze. *Primus Windpower.*
[5]   (2013) Spec Sheet - Ampair turbine. *Ampair Energy Ltd.*
[6]   J. Bartl, "Calibration of Pressure Transducer Magda," T. K. Løken, Ed., ed, 2015.
[7]   R. J., S. Müller, S. Kunz, B. Huguenin-Landl, C. Studer, D. Klauser, *et al.*, "Meteonorm Handbook Part I: Software," *Meteotest,* 2014.
[8]   (2009) Data sheet - Sunways Solar Cells. *Sunways Photovoltaic Technology.*